Modelling of devices for optoelectronic applications: The quantum confined Stark effect and self-electrooptic effect devices

Eckehard SCHÖLL

Institut für Theoretische Physik, Technische Universität BERLIN
Hardenbergstraße 36, 10623 Berlin, GERMANY
email: schoell@physik.tu-berlin.de, Tel. +49 30 314-23500, FAX -21130

Abstract

Electro-optical effects, such as the Franz-Keldysh effect in bulk materials or the quantum confined Stark effect in quantum well structures, lead to strong optoelectronic nonlinearities which form the basis for optical modulators and optically bistable devices. They result from a modification of the optical absorption properties by an applied electric field and are particularly pronounced in the case of low dimensional semiconductors. We review theoretical modelling and computer simulations of such optoelectronic devices in particular for ZnSe based quantum well structures, where excitonic features dominate even at room temperature. The field dependent absorption spectra are calculated by a many-body theory including the full electron-electron interaction. The transition from the quantum confined Stark effect, which is found for well widths smaller than the exciton Bohr diameter, to the Franz-Keldysh effect, which corresponds to the limit of wide wells, is studied. Optical bistability and switching is found in R-SEED and D-SEED configurations, and the optimization of the device performance is discussed.

85.60.Bt, 42.65.Pc, 78.66.Hf

1. Introduction

Electro-optic effects in semiconductor quantum well structures have been the focus of intensive research because of their potential applications to optoelectronic devices, such as electro-optical modulators or bistable switches. Among these effects, the Quantum Confined Stark Effect [1] (QCSE) has recently received particular attention. If a quantum well (QW) is placed in a strong electric field perpendicular to the quantum well plane, the electronic levels are shifted such that the interband absorption experiences a red

shift, and the wave functions are distorted such that their overlap decreases and the oscillator strength is diminished. Accordingly, the absorption coefficient is reduced. As a consequence, the red shift of the absorption edge is accompanied by a pronounced decrease of the absorption peak value. This effect can be used for an optically bistable device by connecting the quantum well structure to a load circuit, which provides a feedback of the field-dependent absorption to the voltage drop across the device. Such self-electrooptic effect devices [3] (SEED) act as bistable switches and optical modulators.

An essential feature of the QCSE is the persistence of the excitonic absorption peak up to much higher fields than observed for the Stark shift in bulk material. The latter effect is caused by the rapid field-ionization of the bulk exciton, whereas the barriers in quantum well structures prevent field-ionization up to high electric fields. Therefore, the exciton Bohr radius must be compared to the quantum well width. If the well width is larger than the exciton Bohr diameter, the excitonic features can be regarded to be bulk-like, while the QCSE will govern the electric-field dependence of quantum wells narrower than the exciton Bohr diameter. If the Coulomb interaction is neglected, the analysis of the quantum confined Stark effect leads to the quantum confined Franz-Keldysh effect between the discrete levels of the well and passes over to the bulk Franz-Keldysh effect in the limit of further increased well width [2].

SEEDs have triggered a lot of investigations and resulted in a variety of new devices for optical switching and processing applications reviewed, e.g., in Ref.4, 5 Most previous work has focussed on the AlGaAs/GaAs material system, for which detailed theoretical models have been developed [6]. ZnSe-based SEED structures [7, 8, 9, 10] have recently become of interest because of the need to integrate ZnSe-based laser diodes with passive components like modulators and switches in the blue-green spectral range. The modeling of electro-absorption in these materials, however, is much more difficult due to the stronger Coulomb interaction and excitonic features, since the standard approximations[6] are not appropriate in this case. A quantum mechanical model for electric field dependent absorption in ZnCdSe/ZnSSe quantum wells, which fully takes account of the Coulomb interaction leading to intersubband coupling and strong excitonic effects and can describe the transition from two-dimensional to three-dimensional behavior, has recently been developed [11, 12].

The SEED is a single or multiple quantum well embedded in the intrinsic layer of a p-i-n structure in combination with a simple electrical circuit. Because of the doping, an intrinsic electric field drops across the quantum well having a strength of approximately the built-in voltage U_{bi} divided by the intrinsic layer width z_i. However, the field is modified by the voltage drop across the device, which depends on the electrical circuit. If the quantum well is illuminated, two effects occur. First, the QW acts as a *modulator* because the absorption coefficient changes according to a variation of the voltage drop. Second, the QW acts as a *photodetector*, because each absorbed photon creates an electron and a hole, resulting in the photocurrent. The relation between the voltage and photocurrent is given by the equation of the electrical circuit. If the operating wavelength is chosen to match the excitonic absorption peak for low fields, then for high electric fields the absorption peak is detuned from the operating wavelength thus leading to a low absorption

636

coefficient. If the operating wavelength is chosen off the exciton resonance peak at zero field, then with increasing field the absorption coefficient may be tuned into resonance; thus increasing up to a maximum and subsequently decreasing again.
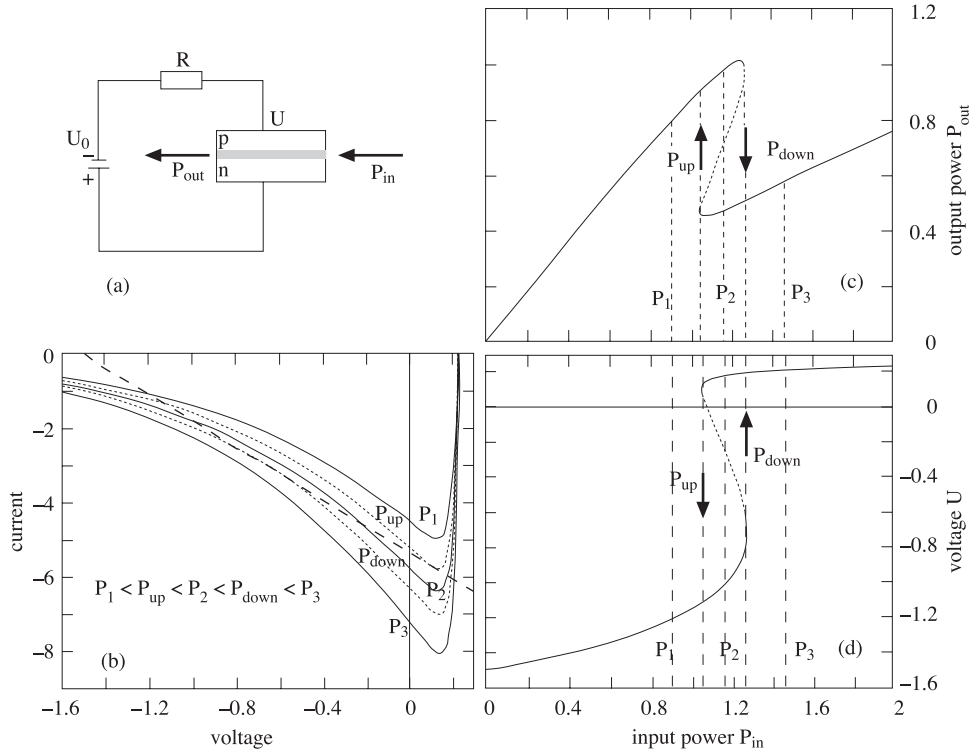

Figure 1. The R-SEED: (a) electrical circuit, (b) load line analysis for five different optical input powers, (c) optical output power P_{out} vs. input power P_{in}, (d) device voltage U vs. P_{in}. (Schematic)

To build a SEED, the p-i-n structure is connected in series with a constant reverse bias U_0 and a load resistor R (*R-SEED*), as shown in Figure 1(a), or a reverse biased photodiode (*D-SEED*), as shown in Figure 2(a). Since the resistance of the reverse biased p-i-n-junction is generally larger than the load resistance, the voltage drops mainly across the device increasing the field strength and, as a consequence, decreasing the absorption coefficient below the equilibrium value. To operate the SEED, first a low optical input power P_{in} is switched on. This results in low optical absorption, and the SEED is nearly transparent. Increasing P_{in} leads to an increasing photocurrent due to the optically generated carriers.

The reverse bias voltage $U_0(< 0)$, the voltage drop at the p-i-n-structure U, and the current J through the device are related according to Kirchhoff's law

$$U_0 = U + RJ \tag{1}$$

637

The current through the device, in a simple approximation, is given by

$$J(P_{in}, U) = -e\frac{P_{in}}{\hbar\omega}(1 - e^{-\alpha(F)L}) + J_r(-1 + e^{eU/k_BT}) \qquad (2)$$

The first contribution is the photocurrent with the field dependent absorption coefficient $\alpha(F)$ (at frequency ω) and the absorption length L, e is the elementary charge. It can be derived from the optical generation rate per unit volume $G = \frac{P(x)}{A}\frac{\alpha}{\hbar\omega}$ by integrating over the cross section A and the absorption length L which is given for a waveguide configuration by the optical confinement factor Γ^{WG} times the waveguide length L^{WG}.

The electric field F is given approximately by

$$F = (U_{bi} - U)/z_i \qquad (3)$$

.

The second contribution to eq. (2) is the dark current-voltage characteristic of the p-i-n-structure, where J_r is the reverse saturation current, T is the temperature, and k_B is Boltzmann's constant.

It follows from eq. (2) that the resistance of the structure is decreased with increasing optical input power. This results in a reduction of the voltage drop U across the structure according to Kirchhoff's law (1). Consequently, the electric field strength in the quantum well decreases and, therefore, the absorption coefficient increases, which, in turn, increases the photocurrent. This positive feedback leads to a switching from the nearly transparent state into a highly absorbing state, at an input power P_{down}. The device switches back when the input power is sufficiently decreased. However, since the device is now in a highly absorbing state, this occurs at a lower input power P_{up}. For input powers P in the range $P_{up} < P < P_{down}$ the device can be in two stable states, one of which is nearly transparent and one which is highly absorbing. This yields hysteresis when the optical input power is swept up and down, respectively.

For a more detailed discussion of the R-SEED the current-voltage characteristic of the device according to eq. (2) is schematically plotted in Figure 1(b) for five different optical input powers P_1, P_2, P_3, P_{up}, and P_{down}. Solutions of Kirchhoff's equation are the intersection points of the characteristic with the load line (dashed). For P_1 and P_3 there exists only one intersection point, representing one (stable) solution. For P_2 there are three intersections with the load line, indicating that the SEED has three stationary states (two of which are stable). In Figure 1 d, the device voltage U corresponding to these operating points is plotted as a function of the optical input power P_{in}. From the absorption coefficient associated with the respective voltages, the P_{out} vs. P_{in} characteristic Figure 1(c) is found: At the critical input powers P_{in} and P_{out}, the voltage drop at the device switches, and again hysteresis is found.

Replacing the resistor with a conventional photodiode, gives the D-SEED. In Figure 2, the circuit and the electro-optical characteristics are schematically shown. The advantage of the D-SEED configuration compared to the R-SEED is the possibility to tune the 'load curve', which is determined by the current-voltage characteristic of the external photodiode, by changing the optical power by which the photodiode is illuminated.

Further, the bistable range can be enlarged while the bias voltage U_0 is reduced and the contrast is significantly improved.
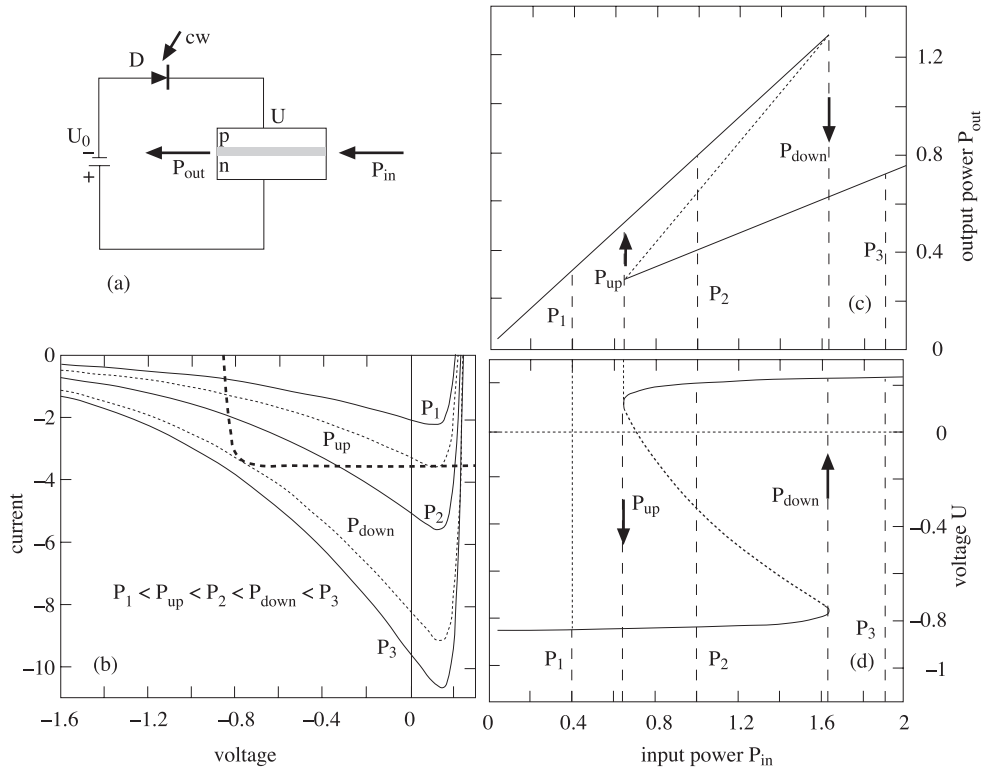

Figure 2. The D-SEED: (a) electrical circuit, (b) circuit analysis for five different optical input powers, (c) optical output power P_{out} vs. input power P_{in}, (d) device voltage U vs. P_{in}. (Schematic)

2. Electric-field dependent absorption in quantum wells

The electric-field dependent absorption in GaAs/AlGaAs multiple quantum well structures has been successfully modeled by a decomposition of the total absorption coefficient into distinct contributions of pairs of levels, each correlated with an exciton[6]. However, this approach which neglects intersubband coupling requires that the Coulomb interaction is only a small perturbation of the confinement potential forming the quantum well. This condition is well satisfied in the case of GaAs/AlGaAs heterostructures but is violated for ZnSe-based structures, due to the much stronger Coulomb interaction and larger exciton binding energy. Typical exciton binding energies are of the order of 17 meV in GaAs- and 80 meV in ZnSe-based quantum wells, respectively.

As a result, the coupling of the different discrete levels as well as their coupling with

bulk continuum states above the quantum well barrier by means of the Coulomb interaction turns out to be essential. Applying the density matrix formalism in real space [13] we have calculated the absorption coefficient for a wide range of applied fields and quantum well widths covering the transition from two- to three-dimensional behavior. Details of the calculations are given in Ref.12. First, the Schrödinger equation for the coherent interband amplitude, i.e., the polarization induced by the exciting electromagnetic wave, is set up. In order to solve this equation, a series expansion of the polarization in the basis of the eigenfunctions of the one-dimensional Schrödinger equation for the quantum well potential is performed including *all* Coulomb matrix elements. Finally, the absorption coefficient is related to the imaginary part of the polarization Y^{vc} according to

$$\alpha(Z,\omega) = \frac{\omega}{cn_r} \, Im \, \frac{2M_0 Y^{vc}(Z,\omega)}{\epsilon_0 E_\omega} \tag{4}$$

where M_0 is the dipole matrix element, E_ω is the complex amplitude of the electromagnetic wave of frequency ω, c is the velocity of light and n_r is the real refractive index. As a consequence of the spatial inhomogeneity in the vertical direction due to the electric field and the confinement potential, the polarization, and thus the the *local* absorption coefficient, emerge as a function of the exciton center of mass coordinate Z. To relate it to the measured absorption coefficient, it has to be integrated over the Z-direction for a symmetric sample with surfaces at $Z = \pm L^z/2$ and normalized by the width L^{QW} of the quantum well according to

$$\alpha = \frac{1}{L^{QW}} \int\limits_{-L^z/2}^{+L^z/2} \alpha(Z,\omega)dZ. \tag{5}$$

If the direction of the light beam is perpendicular to the quantum well layer, the absorption length is extremely short (equal to the width of the well). To enlarge the absorption length, often multiple quantum well structures are used where the absorption length is the well width multiplied by the number of periods. Alternatively, an increased absorption length can also be obtained by the use of an optical waveguide [14] with a quantum well embedded in the center of the waveguide core. Then, the transmission is in the QW plane (x-direction) and the absorbing length is the whole sample length. The optical power

$$P(x) = P_{in}exp(-\alpha x) \tag{6}$$

is exponentially attenuated in the propagating direction along the waveguide.

We have performed simulations for ZnCdSe quantum wells with a width of L^{QW}=3, 5, 10, and 15nm and different applied electric fields, and obtained good agreement with the experiment [12]. Starting from a nearly two-dimensional situation, Figure 3 (a) shows the (averaged) absorption coefficient α for a well width of 3nm for fields up to 360 kV/cm. The field dependent changes can obviously be attributed to the *quantum confined Stark effect*. With increasing field the excitonic resonance shifts to lower photon

energies accompanied by a strong decrease in the peak value together with a field induced broadening of the peak width. At about 360kV/cm the excitonic peak disappears and the absorption coefficient is reduced approximately to half of the peak value at zero-field.

For the 5nm quantum well, the simulation results are depicted in Figure 3(b). The QCSE can clearly be identified. With increasing field the excitonic resonance shifts to lower photon energies accompanied by a strong decrease in the peak value together with a field induced broadening of the peak width. On the high energy shoulder, an additional peak arises with increasing electric field. While the absorption peak at zero-field is due to the hole ground state to electron ground state transition, this new peak is caused by transitions from the second level of the hole to the ground state of the electron. This additional transition is forbidden at zero field because of parity reasons. With increasing electric field, the wavefunctions become distorted, hence the overlap of the wavefunctions involved in the forbidden transitions does not vanish any more.

From the dependence of the absorption spectra on the electric field strength it can be deduced that for wider wells a transition from a two-dimensional to a three-dimensional behavior occurs: The spectra for a well width of, e.g., 10nm show excitonic peaks, however, a pronounced red shift cannot be found due to a rapid field induced dissociation of the exciton which results in a strong broadening of the resonances with increasing electric field (Figure 3(c)). For a quantum well width of 15nm (Figure 3 (d)), bulk-like behavior with respect to the dimensionality of the exciton is found: The excitonic peak at zero field vanishes before any peak shift can be seen. However, with respect to the density of states, the bulk limit is not reached and hence the absorption spectra for the 15nm quantum well can be associated with the *quantum confined Franz-Keldysh regime*[2]. Even wider wells would correspond to the transition from a two-dimensional to a fully three-dimensional center-of-mass motion of the exciton.

The absorption coefficient is plotted versus field in Figure 4 for various photon energies and a smaller exciton-phonon linewidth Γ (solid lines). By a variation of the photon energy, the maximum of the absorption coefficient can be adjusted to any field strength. For larger linewidth (dotted line) and larger well width (dashed line) the field modulation of the absorption coefficient becomes weaker; hence narrow wells and a small linewidth (long dephasing time) are favorable for applications as electrooptic modulators.

3. Self-Electrooptic Effect Devices

We shall now apply the preceding results to the modeling of a self-electrooptic effect device. To model the SEED operation, the well width is chosen to be $L^{QW} = 5nm$ as an example for two-dimensional structures, and 10nm as an example for the bulk-like structures. The following simulations are performed for a waveguide configuration [16].

At first, the 5nm quantum well is investigated. The calculated device voltage is plotted versus the optical input power P_{in} for various optical frequencies in Figure 5. The arrows indicating the switching cycles are given for two exemplary frequencies ($\hbar\omega = 2.465eV$ and $2.480eV$).

The influence of the operational control parameters $E_{ph} = \hbar\omega$, U_0, and P_{in} can now be

analyzed for fixed structural parameters. The variation of the frequency strongly alters the highly absorbing state since it shifts the peak in the absorption spectrum (cf. Figure 4) while the (almost transparent) high-field absorption coefficient is only slightly affected.
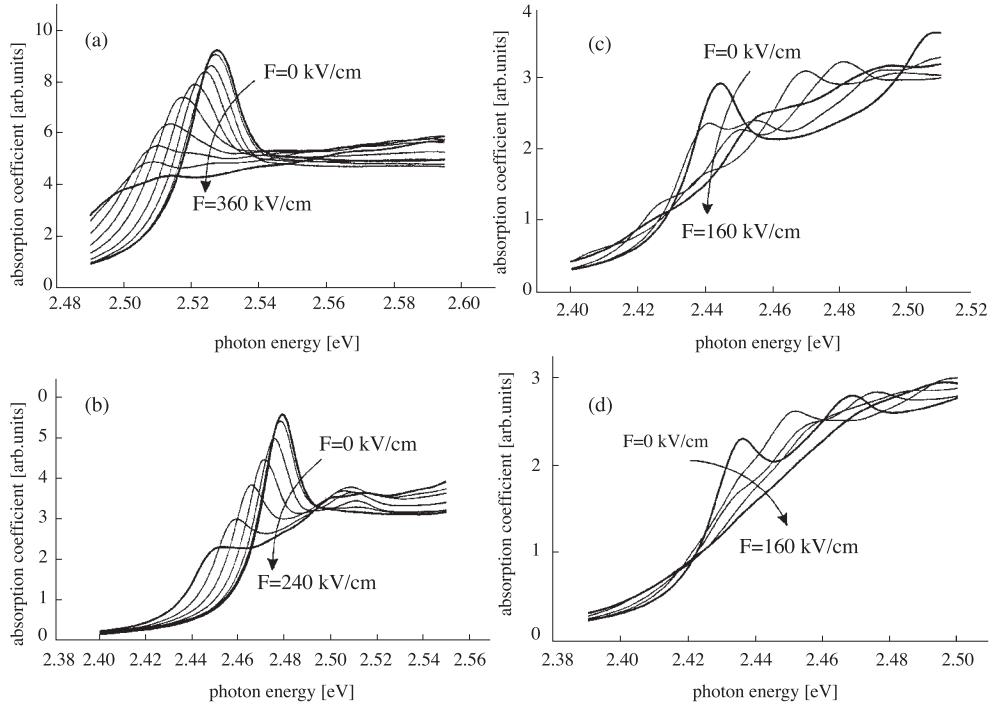

Figure 3. Calculated electric field dependence of the absorption coefficient α for different widths of the $Zn_{0.7}Cd_{0.3}Se$ quantum well: (a) 3nm, (b) 5nm, (c) 10nm, (d) 15nm. Different curves correspond to different electric field strengths increasing with the arrow in steps of 40 kV/cm (Linewidth Γ=10meV).

Next, the SEED characteristics will be investigated in dependence on the reverse bias U_0 for an operation frequency $\hbar\omega = 2.475eV$ corresponding to an absorption peak close to the intrinsic field at the built-in voltage U_{bi}. Figure 6(a) shows the electro-optical characteristics for different bias voltages U_0. Bistability is now present for all values of the bias voltage. The resulting optical input-output characteristic (Figure 6 (b)) exhibits optical bistability between an almost transparent and a highly absorbing state. The width of the bistability regime can be conveniently controlled by the bias voltage. The width of the bistability regime as well as the switching contrast and the threshold input power may also be tuned by the waveguide length [11, 16].

Multiple bistability and even multistability can be obtained with structures that show more than one maximum in the field-dependent absorption coefficient. This requires small values for the linewidth in order to resolve the different peaks. At first, the R-SEED is

discussed for a quantum well of width $10nm$ with $\hbar\omega = 2.440eV$ (Figure 7(a)). Due to the two maxima in the field-dependent absorption coefficient (Figure 7 (b)), bistability can be observed twice.
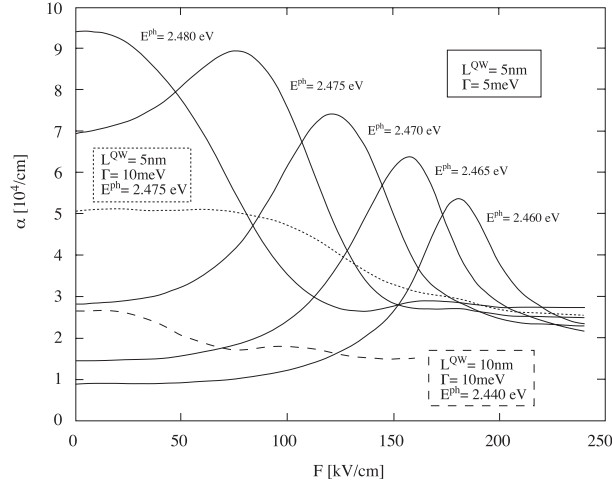

Figure 4. Calculated absorption coefficient as function of the electric field strength. Solid lines: $L^{QW} = 5nm$, $\Gamma = 5meV$, $E^{ph} = 2.460...2.480eV$. Dotted line: $L^{QW} = 5nm$, $\Gamma = 10meV$, $E^{ph} = 2.475eV$. Dashed line: $L^{QW} = 10nm$, $\Gamma = 10meV$, $E^{ph} = 2.440$.
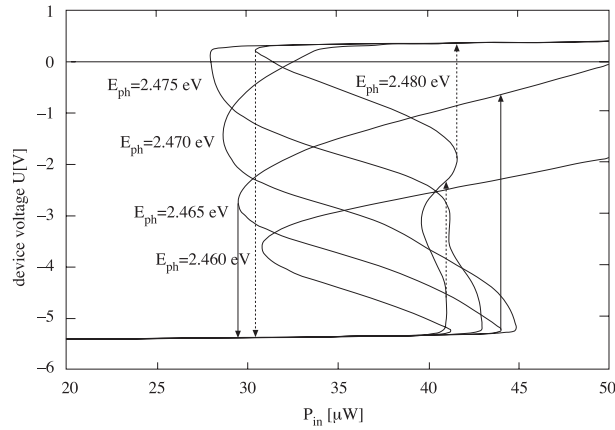

Figure 5. Device voltage U vs. optical input power P_{in} for a D-SEED with bias voltage $U_0 = -5V$ and different photon energies $E_{ph} = \hbar\omega$. $P_{in} = 50\mu W$, $L^{QW} = 5nm$, $z_i = 300nm$, $L^{WG} = 20\mu m$, $\Gamma = 5meV$, $\Gamma^{WG} = 0.02$, reverse saturation current of SEED $J_r = 10pA$. Photodiode: $J_{sc} = 10\mu A$, $J_r = 1pA$.
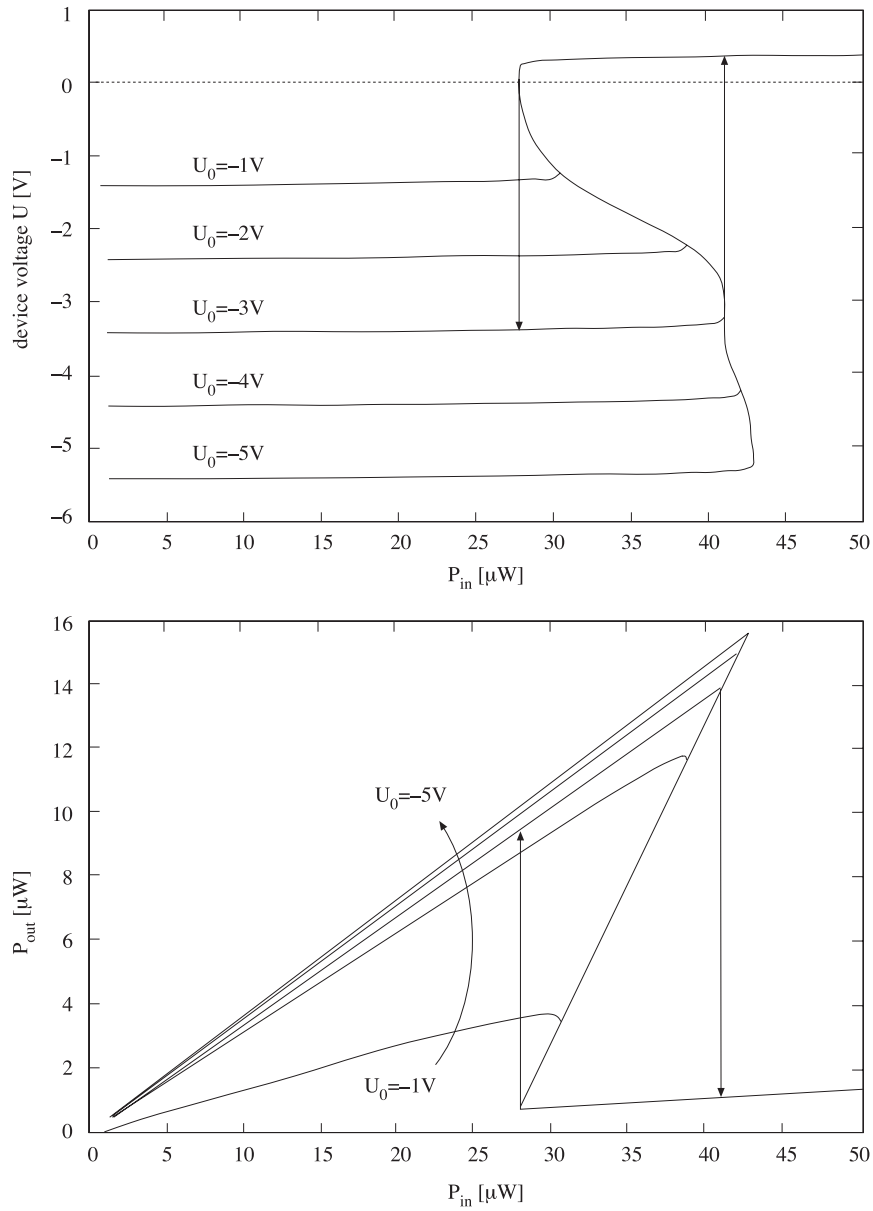
643

Figure 6. (a) Device voltage U vs. optical input power P_{in} for different D-SEED bias voltages U_0. (b) Optical output power P_{out} vs. input power P_{in} for different D-SEED bias voltages $U_0 = -1, -2, -3, -4, -5V$. The arrows denote an exemplary switching cycle at $U_0 = -3V$. ($E_{ph} = 2.475eV$, other parameters as in Figure 5.)
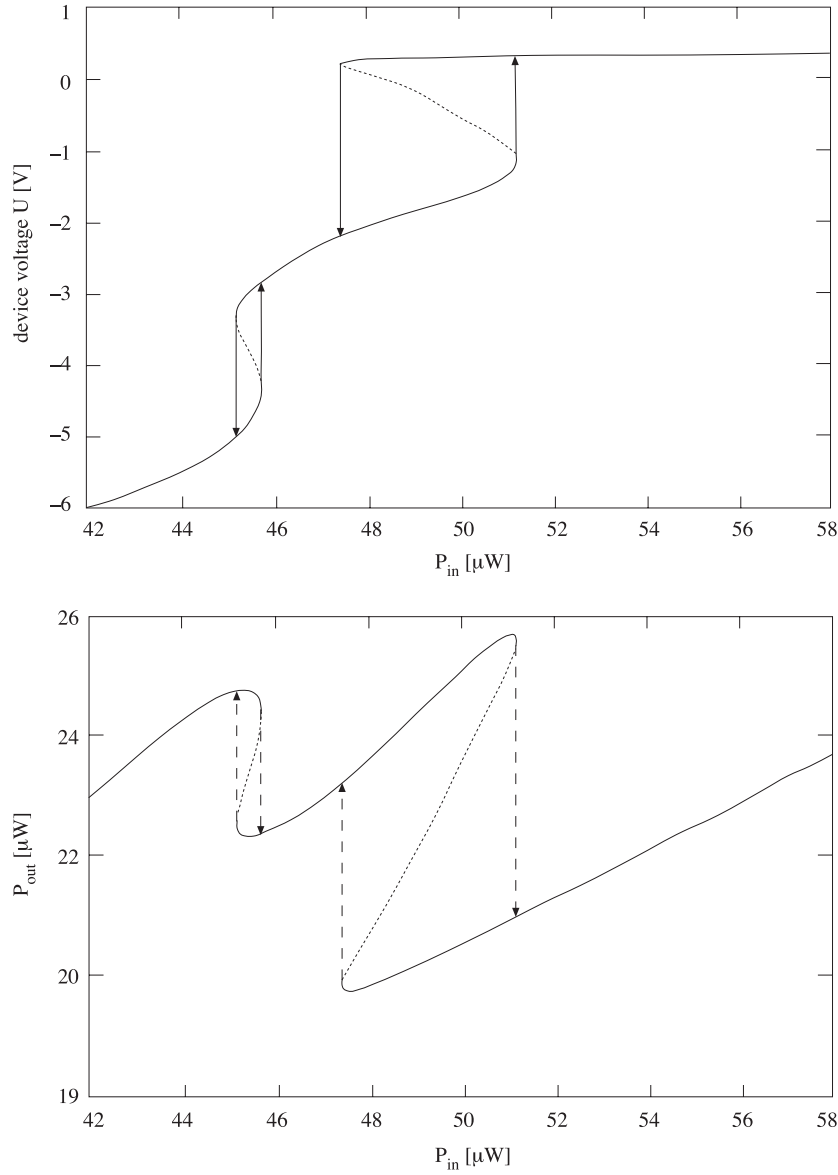
Figure 7. (a) Device voltage U vs. P_{in} for a R-SEED. (b) Optical output power P_{out} vs. P_{in}. ($E_{ph} = 2.440meV$, $L^{QW} = 10nm$, $z_i = 500nm$, $L^{WG} = 20\mu m$, $\Gamma = 10meV$, $R = 2M\Omega$, $U_0 = -20V$.)

Bistability related to the high-field maximum of the absorption coefficient (second-hole to first-electron-level resonance) can be found at input powers $P_{in} \approx 45.5\mu W$ while bista-

bility related to the low-field maximum (electron-hole ground level resonance) is observed at $P_{in} \approx 50 \mu W$. The corresponding optical input-output characteristic is presented in Figure 7(b), again both subsequent hysteresis cycles are visible.

The same analysis can be performed for the D-SEED configuration. In this case, the two well separated bistability regimes which are present in case of the R-SEED merge, leading to *tristability* [11, 16].

4. Conclusions

In this paper we have reviewed computer simulations of self-electrooptic effect devices in different circuit environments (D-SEED and R-SEED). Optical bistability and even multiple switching cycles are predicted from the electrooptical and optical input-output characteristics for a wide range of operating conditions. The dependence upon the optical frequency, bias voltage, length of the waveguide, and quantum well width is discussed. Our work is founded on a microscopic model of the electric field dependent absorption in ZnCdSe/ZnSSe quantum well structures, which takes full account of Coulomb induced intersubband coupling. Because of much stronger Coulomb effects, the physical nature of electroabsorption in wide gap materials, including the transition from two-dimensional to bulk behavior, is entirely different from that in GaAs/AlGaAs structures where the Coulomb interaction may be treated as a small perturbation. Strong Coulomb interaction results in a significant exciton binding energy and, thus, in a small exciton Bohr radius, and a sharp excitonic absorption peak even at room temperature. A well width smaller than the (bulk) exciton diameter results in a two-dimensional exciton, i.e., the relative motion of the electron-hole pair is confined to the well plane. At larger well width, the relative motion is essentially three-dimensional, whereas the center-of-mass motion is still restricted to the plane of the quantum well, and the density of states is still two-dimensional.

For narrow wells of the order of $5 nm$ a pronounced QCSE occurs which leads to a strong modulation of the absorption coefficient with electric field. This is favorable for the operation of a SEED since it yields a large contrast of the optical switching cycle, provided that the optical frequency is chosen close to the peak of the absorption coefficient. The bistability range can be maximized by applying a large negative bias voltage. In view of applications for room temperature operation, a small exciton-phonon coupling is desirable in order to minimize the temperature induced broadening of the excitonic peak; this again favors narrow wells. Choosing the optical operating frequency close to the exciton resonance at the intrinsic field (which may be quite high in a p-i-n structure) enhances the electrooptic modulation of the absorption coefficient, and hence the switching contrast of the SEED. A longer waveguide also increases the contrast and shifts the bistability regime to smaller input power, but it reduces the width of the bistability regime and the absolute value of the transmission change.

Since the difference between conventional models and the advanced model presented here are physically caused by the strong Coulomb coupling typical for wide-gap materials with a small dielectric constant, our advanced model applies not only to ZnCdSe/ZnSSe

646

structures but to a much larger class of wide-gap materials. It offers the convenient possibility to treat SEED operation up to very high electric fields and optimize their performance. The physical interest in these materials is strongly motivated by their potential application as modulators and switches in future integrated optoelectronics in the blue-green range.

Acknowledgements

References

[1] D. A. B. Miller, D. S. Chemla, T. C. Damen, A. C. Gossard, W. Wiegmann, T. H. Wood, and C. A. Burrus, Phys. Rev. Lett. **53**, 2173 (1984).

[2] D. A. B. Miller, D. S. Chemla, and S. Schmitt-Rink, Phys. Rev. B **33**, 6976 (1986).

[3] D. A. B. Miller, D. S. Chemla, T. C. Damen, A. C. Gossard, W. Wiegmann, T. H. Wood, and C. A. Burrus, Appl. Phys. Lett. **45**, 13 (1984).

[4] D. A. B. Miller, Opt. Quantum Electron. **22**, S61 (1990).

[5] A. L. Lentine and D. A. B. Miller, IEEE J. Quant. El. **29**, 655 (1993).

[6] P. J. Mares and S. L. Chuang, J. Appl. Phys. **74**, 1388 (1993).
Jap. J. Appl. Phys. Suppl. **34**, 15 (1995).

[7] S. Y. Wang, Y. Kawakami, J. Simpson, H. Stewart, K. A. Prior, and B. C. Cavenett, Appl. Phys. Lett. **62**, 1715 (1993).

[8] P. V. Giugno, M. D. Vittorio, R. Rinaldi, R. Cingolani, F. Quaranta, L. Vanzetti, L. Sorba, and A. Franciosi, Phys. Rev. B **54**, 16934 (1996).

[9] W. Ebeling, B. S. Ryvkin, J. Gutowski, K. Schüll, B. Jobst, and D. Hommel, J. Crystal Growth **159**, 893 (1996).

[10] W. Ebeling, D. Merbach, M. Behringer, M. Fehrer, P. Michler, J. Gutowski, E. Schöll, and D. Hommel, J. Crystal Growth **184/185**, 706 (1998).

[11] D. Merbach, *Electric Field Dependent Absorption of ZnSe-based Quantum Wells and Application to Optically Bistable Devices* Ph.D. Thesis, Technical University of Berlin (Wissenschaft und Technik Verlag, Berlin, 1998).

[12] D. Merbach, E. Schöll, W. Ebeling, P. Michler, and J. Gutowski, Phys. Rev. B, 58, 10709 (1998).

[13] A. Stahl and I. Balslev, *Electrodynamics of the Semiconductor Band Edge* (Springer, Berlin, 1987).

[14] T. H. Wood, J. Lightwave Technol. **6**, 743 (1988).

[15] E. Schöll, *Nonequilibrium Phase Transitions in Semiconductors*, vol. 35 of *Springer Series in Synergetics* (Springer, Berlin, 1987).

[16] D. Merbach, E. Schöll, and J. Gutowski, J. Appl. Phys. 85, 7051 (1999).